

General Disclaimer

One or more of the Following Statements may affect this Document

- This document has been reproduced from the best copy furnished by the organizational source. It is being released in the interest of making available as much information as possible.
- This document may contain data, which exceeds the sheet parameters. It was furnished in this condition by the organizational source and is the best copy available.
- This document may contain tone-on-tone or color graphs, charts and/or pictures, which have been reproduced in black and white.
- This document is paginated as submitted by the original source.
- Portions of this document are not fully legible due to the historical nature of some of the material. However, it is the best reproduction available from the original submission.

OPTICAL TRANSFER FUNCTION

OF

NTS-1 RETROREFLECTOR ARRAY

(NASA-CR-140667) OPTICAL TRANSFER
FUNCTION OF NTS-1 RETROREFLECTOR ARRAY
(Smithsonian Astrophysical Observatory)
56 p HC \$4.25

CSCL 20F

N75-10773

Unclas

63/74 51099

Technical Report
RTOP 161-05-02

Grant NGR 09-015-002
Supplement No. 57

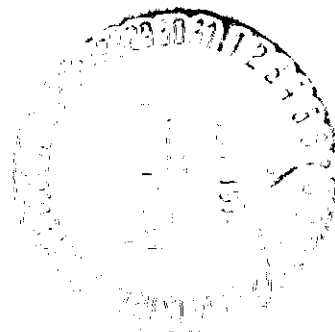
Author: David Arnold

October 1974

Prepared for
National Aeronautics and Space Administration
Washington, D. C. 20546

Smithsonian Institution
Astrophysical Observatory
Cambridge, Massachusetts 02138

The Smithsonian Astrophysical Observatory
and the Harvard College Observatory
are members of the
Center for Astrophysics



OPTICAL TRANSFER FUNCTION
OF
NTS-1 RETROREFLECTOR ARRAY

Technical Report
RTOP 161-05-02

Grant NGR 09-015-002
Supplement No. 57

Author: David Arnold

October 1974

Prepared for
National Aeronautics and Space Administration
Washington, D. C. 20546

Smithsonian Institution
Astrophysical Observatory
Cambridge, Massachusetts 02138

The Smithsonian Astrophysical Observatory
and the Harvard College Observatory
are members of the
Center for Astrophysics

TABLE OF CONTENTS

<u>Section</u>	<u>Page</u>
ABSTRACT	v
1 INTRODUCTION	1
2 CUBE-CORNER SPECIFICATIONS	3
3 GEOMETRY OF ARRAY	5
4 SIGNAL-STRENGTH COMPUTATION	13
5 METHOD OF COMPUTING TRANSFER FUNCTION	15
6 GAIN FUNCTION	17
7 ACTIVE REFLECTING AREA	35
8 RANGE CORRECTION	37
9 PULSE SPREADING	39
10 VARIATIONS IN PULSE SHAPE DUE TO OPTICAL COHERENCE	41
11 VARIATIONS IN PULSE CENTROID DUE TO OPTICAL COHERENCE .	53
12 ACCURACY OF RANGE CORRECTION.	57
13 ACKNOWLEDGMENTS	59

PRECEDING PAGE BLANK NOT FILMED

ILLUSTRATIONS

<u>Figure</u>		<u>Page</u>
1	Array coordinate system	6
2	Coordinate system of incident beam	18
3	Coherent pulse shapes	42

TABLES

<u>Table</u>		<u>Page</u>
1	Retroreflector positions	7
2	Gain-function matrices for various incidence angles and two wave-lengths	19
3	Active reflecting area as a function of angle of incidence.	36
4	Range correction	37
5	Pulse spread	40
6	Pulse strength and centroid	41
7a	Coherent range variations, with equal weighting	54
7b	Coherent range variations, weighted by signal strength	55

ABSTRACT

This report covers work done under the Office of Applications supplement to NASA Grant NGR 09-015-002. An optical transfer function has been computed for the retro-reflector array carried by the NTS-1 satellite (1974 56A), formerly called Timation III. Range corrections are presented for extrapolating laser range measurements to the center of mass of the satellite. The gain function of the array has been computed for use in estimating laser-echo signal strengths.

OPTICAL TRANSFER FUNCTION
OF
NTS-1 RETROREFLECTOR ARRAY

RTOP Special Report 161-05-02

1. INTRODUCTION

The calculations presented here were done by using computer programs developed under two previous NASA grants.* The final report for Grant NGR 09-015-164 presents analyses done for the Lageos satellite, while Grant NGR 09-015-196 gives results calculated for the BE-B, BE-C, Geos 1, Geos 2, D1C, D1D, and Pecos satellites. A complete description of the equations used in these computer programs is to be published as a Smithsonian Astrophysical Observatory Special Report.

Data on the NTS-1 retroreflector array were obtained from Goddard Space Flight Center (GSFC), the Naval Research Laboratory, and Fairchild Space and Electronics Company.

This report contains technical data on the array and the optical transfer function of the array.

* Grant NGR 09-015-164, Use of a Passive Stable Satellite for Earth Physics Applications, and Grant NGR 09-015-196, Calculation of Retroreflector Array Transfer Functions.

2. CUBE-CORNER SPECIFICATIONS

The cube corners have hexagonal entrance faces with a width of 15 mm across flats and a length from vertex to face of $15/\sqrt{2} = 10.61$ mm. The size is chosen to maximize the strength of the return signal at an angle from the retroreflection direction equal to the velocity aberration of the satellite.* The material is fused silica with silvered back reflecting faces. Testing done on the cube corners at GSFC indicates that they are all very close to diffraction-limited.

PRECEDING PAGE BLANK NOT FILMED

* "Design of Retrodirector Arrays for Laser Ranging of Satellites," by Peter O. Minott, Goddard Space Flight Center X-723-74-122, 1974.

3. GEOMETRY OF ARRAY

The array consists of 420 cube corners, all with the same orientation in a single plane facing the earth. The satellite is gravity stabilized. The distance from the center of mass of the spacecraft to the front face of the retroreflectors is 13.6 ± 0.03 inches (0.3454 m). Table 1 lists the X and Y coordinates in meters of the center of the front face of each cube corner, and the orientation of the X and Y axes is shown in Figure 1. The first two columns in the table are the indices giving the row number and the position within the row, respectively. The rows are numbered from top to bottom, and the position within the row, from left to right.

PRECEDING PAGE BLANK NOT FILMED

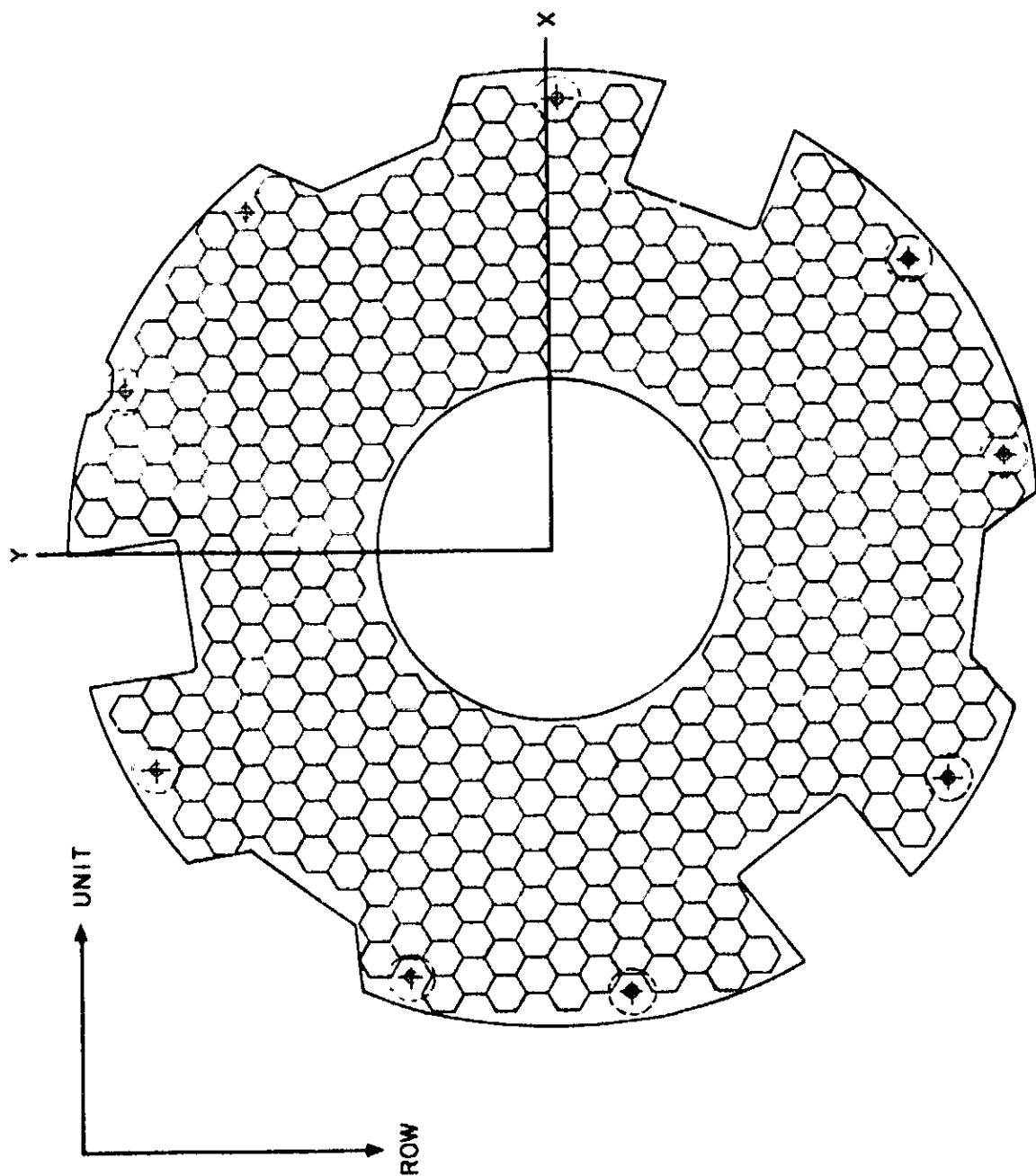


Figure 1. Array coordinate system.

Table 1. Retroreflector positions (in meters).

ROW	UNIT	X	Y	ROW	UNIT	X	Y
1	1	.01595	.20262	6	8	-.00798	.13355
1	2	.03190	.20262	6	9	.00798	.13355
2	1	-.07178	.18880	6	10	.02393	.13355
2	7	.02393	.18880	6	11	.03988	.13355
2	8	.03988	.18880	6	12	.05583	.13355
2	9	.05583	.18880	6	13	.07178	.13355
3	1	-.07976	.17499	6	14	.08773	.13355
3	2	-.06380	.17499	6	15	.10368	.13355
3	7	.01595	.17499	6	16	.11963	.13355
3	8	.03190	.17499	6	17	.13559	.13355
3	9	.04785	.17499	7	1	-.12761	.11973
3	10	.06380	.17499	7	2	-.11166	.11973
3	11	.07976	.17499	7	3	-.09571	.11973
3	12	.09571	.17499	7	4	-.07976	.11973
4	1	-.11963	.16117	7	5	-.06380	.11973
4	2	-.10368	.16117	7	6	-.04785	.11973
4	3	-.08773	.16117	7	7	-.03190	.11973
4	4	-.07178	.16117	7	8	-.01595	.11973
4	10	.02393	.16117	7	9	0.00000	.11973
4	11	.03988	.16117	7	10	.01595	.11973
4	12	.05583	.16117	7	11	.03190	.11973
4	13	.07178	.16117	7	12	.04785	.11973
4	14	.08773	.16117	7	13	.06380	.11973
4	15	.10368	.16117	7	14	.07976	.11973
4	16	.11963	.16117	7	15	.09571	.11973
5	1	-.12761	.14736	7	16	.11166	.11973
5	2	-.11166	.14736	7	17	.12761	.11973
5	3	-.09571	.14736	7	18	.14356	.11973
5	4	-.07976	.14736	7	19	.15951	.11973
5	5	-.06380	.14736	8	1	-.13559	.10592
5	6	-.04785	.14736	8	2	-.11963	.10592
5	7	-.03190	.14736	8	3	-.10368	.10592
5	8	-.01595	.14736	8	4	-.08773	.10592
5	9	0.00000	.14736	8	5	-.07178	.10592
5	10	.01595	.14736	8	6	-.05583	.10592
5	11	.03190	.14736	8	7	-.03988	.10592
5	12	.04785	.14736	8	8	-.02393	.10592
5	13	.06380	.14736	8	9	-.00798	.10592
5	14	.07976	.14736	8	10	.00798	.10592
5	15	.09571	.14736	8	11	.02393	.10592
5	16	.11166	.14736	8	12	.03988	.10592
5	17	.12761	.14736	8	13	.05583	.10592
5	18	.14356	.14736	8	14	.07178	.10592
6	1	-.11963	.13355	8	15	.08773	.10592
6	2	-.10368	.13355	8	16	.10368	.10592
6	3	-.08773	.13355	8	17	.11963	.10592
6	4	-.07178	.13355	8	18	.13559	.10592
6	5	-.05583	.13355	8	19	.15154	.10592
6	6	-.03988	.13355	9	1	-.14356	.09210
6	7	-.02393	.13355	9	2	-.12761	.09210

Table 1 (Cont.)

ROW	UNIT	X	Y	ROW	UNIT	X	Y
9	3	-.11166	.09210	12	1	-.19939	.05066
9	4	-.09571	.09210	12	2	-.18344	.05066
9	5	-.07976	.09210	12	3	-.16749	.05066
9	6	-.06380	.09210	12	4	-.15154	.05066
9	7	-.04785	.09210	12	5	-.13559	.05066
9	8	-.03190	.09210	12	6	-.11963	.05066
9	9	-.01595	.09210	12	7	-.10368	.05066
9	10	0.00000	.09210	12	8	-.08773	.05066
9	11	.01595	.09210	12	9	-.07178	.05066
9	12	.03190	.09210	12	18	.07178	.05066
9	13	.04785	.09210	12	19	.08773	.05066
9	14	.06380	.09210	12	20	.10368	.05066
9	15	.07976	.09210	12	21	.11963	.05066
9	16	.09571	.09210	12	22	.13559	.05066
9	17	.11166	.09210	12	23	.15154	.05066
9	18	.12761	.09210	12	24	.16749	.05066
9	19	.14356	.09210	13	1	-.19141	.03685
10	1	-.18344	.07829	13	2	-.17546	.03685
10	2	-.16749	.07829	13	3	-.15951	.03685
10	3	-.15154	.07829	13	4	-.14356	.03685
10	4	-.13559	.07829	13	5	-.12761	.03685
10	5	-.11963	.07829	13	6	-.11166	.03685
10	6	-.10368	.07829	13	7	-.09571	.03685
10	7	-.08773	.07829	13	8	-.07976	.03685
10	8	-.07178	.07829	13	18	.07976	.03685
10	9	-.05583	.07829	13	19	.09571	.03685
10	10	-.03988	.07829	13	20	.11166	.03685
10	15	.03988	.07829	13	21	.12761	.03685
10	16	.05583	.07829	13	22	.14356	.03685
10	17	.07178	.07829	13	23	.15951	.03685
10	18	.08773	.07829	13	24	.17546	.03685
10	19	.10368	.07829	13	25	.19141	.03685
10	20	.11963	.07829	14	1	-.19939	.02303
10	21	.13559	.07829	14	2	-.18344	.02303
10	22	.15154	.07829	14	3	-.16749	.02303
11	1	-.17546	.06447	14	4	-.15154	.02303
11	2	-.15951	.06447	14	5	-.13559	.02303
11	3	-.14356	.06447	14	6	-.11963	.02303
11	4	-.12761	.06447	14	7	-.10368	.02303
11	5	-.11166	.06447	14	8	-.08773	.02303
11	6	-.09571	.06447	14	19	.08773	.02303
11	7	-.07976	.06447	14	20	.10368	.02303
11	8	-.06380	.06447	14	21	.11963	.02303
11	16	.06380	.06447	14	22	.13559	.02303
11	17	.07976	.06447	14	23	.15154	.02303
11	18	.09571	.06447	14	24	.16749	.02303
11	19	.11166	.06447	14	25	.18344	.02303
11	20	.12761	.06447	14	26	.19939	.02303
11	21	.14356	.06447	15	1	-.19141	.00922
11	22	.15951	.06447	15	2	-.17546	.00922

Table 1 (Cont.)

ROW	UNIT	X	Y	ROW	UNIT	X	Y
15	3	-.15951	.00922	18	20	.11963	-.03222
15	4	-.14356	.00922	18	21	.13559	-.03222
15	5	-.12761	.00922	18	22	.15154	-.03222
15	6	-.11166	.00922	18	24	.18344	-.03222
15	7	-.09571	.00922	18	25	.19939	-.03222
15	19	.09571	.00922	19	1	-.19141	-.04604
15	20	.11166	.00922	19	2	-.17546	-.04604
15	21	.12761	.00922	19	3	-.15951	-.04604
15	22	.14356	.00922	19	4	-.14356	-.04604
15	23	.15951	.00922	19	5	-.12761	-.04604
15	24	.17546	.00922	19	6	-.11166	-.04604
15	25	.19141	.00922	19	7	-.09571	-.04604
16	1	-.19939	-.00460	19	8	-.07976	-.04604
16	2	-.18344	-.00460	19	18	.07976	-.04604
16	3	-.16749	-.00460	19	19	.09571	-.04604
16	4	.15154	-.00460	19	20	.11166	-.04604
16	5	-.13559	-.00460	19	21	.12761	-.04604
16	6	-.11963	-.00460	19	22	.14356	-.04604
16	7	-.10368	-.00460	20	1	-.18344	-.05985
16	8	-.08773	-.00460	20	2	-.16749	-.05985
16	19	.08773	-.00460	20	3	-.15154	-.05985
16	20	.10368	-.00460	20	4	-.13559	-.05985
16	21	.11963	-.00460	20	5	-.11963	-.05985
16	22	.13559	-.00460	20	6	-.10368	-.05985
16	23	.15154	-.00460	20	7	-.08773	-.05985
16	24	.16749	-.00460	20	8	-.07178	-.05985
16	25	.18344	-.00460	20	17	.07178	-.05985
17	1	-.19141	-.01841	20	18	.08773	-.05985
17	2	-.17546	-.01841	20	19	.10368	-.05985
17	3	-.15951	-.01841	20	20	.11963	-.05985
17	4	-.14356	-.01841	20	21	.13559	-.05985
17	5	-.12761	-.01841	21	1	-.19141	-.07367
17	6	-.11166	-.01841	21	2	-.17546	-.07367
17	7	-.09571	-.01841	21	3	-.15951	-.07367
17	19	.09571	-.01841	21	5	-.12761	-.07367
17	20	.11166	-.01841	21	6	-.11166	-.07367
17	21	.12761	-.01841	21	7	-.09571	-.07367
17	22	.14356	-.01841	21	8	-.07976	-.07367
17	23	.15951	-.01841	21	9	-.06380	-.07367
17	24	.17546	-.01841	21	10	-.04785	-.07367
17	25	.19141	-.01841	21	16	.04785	-.07367
18	1	-.18344	-.03222	21	17	.06380	-.07367
18	2	-.16749	-.03222	21	18	.07976	-.07367
18	3	-.15154	-.03222	21	19	.09571	-.07367
18	4	-.13559	-.03222	21	20	.11166	-.07367
18	5	-.11963	-.03222	21	21	.12761	-.07367
18	6	-.10368	-.03222	22	1	-.18344	-.08748
18	7	-.08773	-.03222	22	5	-.11963	-.08748
18	18	.08773	-.03222	22	6	-.10368	-.08748
18	19	.10368	-.03222	22	7	-.08773	-.08748

Table 1 (Cont.)

ROW	UNIT	X	Y	ROW	UNIT	X	Y
22	8	-.07178	-.08748	25	3	-.06380	-.12892
22	9	-.05583	-.08748	25	4	-.04785	-.12892
22	10	-.03988	-.08748	25	5	-.03190	-.12892
22	11	-.02393	-.08748	25	6	-.01595	-.12892
22	12	-.00798	-.08748	25	7	0.00000	-.12892
22	13	.00798	-.08748	25	8	.01595	-.12892
22	14	.02393	-.08748	25	9	.03190	-.12892
22	15	.03988	-.08748	25	10	.04785	-.12892
22	16	.05583	-.08748	25	11	.06380	-.12892
22	17	.07178	-.08748	25	12	.07976	-.12892
22	18	.08773	-.08748	25	13	.09571	-.12892
22	19	.10368	-.08748	25	14	.11166	-.12892
22	20	.11963	-.08748	25	15	.12761	-.12892
23	1	-.11166	-.10130	25	16	.14356	-.12892
23	2	-.09571	-.10130	25	17	.15951	-.12892
23	3	-.07976	-.10130	26	1	-.11963	-.14274
23	4	-.06380	-.10130	26	2	-.10368	-.14274
23	5	-.04785	-.10130	26	3	-.08773	-.14274
23	6	-.03190	-.10130	26	4	-.07178	-.14274
23	7	-.01595	-.10130	26	5	-.05583	-.14274
23	8	0.00000	-.10130	26	6	-.03988	-.14274
23	9	.01595	-.10130	26	7	-.02393	-.14274
23	10	.03190	-.10130	26	8	-.00798	-.14274
23	11	.04785	-.10130	26	9	.00798	-.14274
23	12	.06380	-.10130	26	10	.02393	-.14274
23	13	.07976	-.10130	26	11	.03988	-.14274
23	14	.09571	-.10130	26	12	.05583	-.14274
23	15	.11166	-.10130	26	13	.07178	-.14274
23	16	.12761	-.10130	26	14	.08773	-.14274
23	17	.14356	-.10130	26	15	.10368	-.14274
24	1	-.10368	-.11511	26	16	.11963	-.14274
24	2	-.08773	-.11511	26	17	.13559	-.14274
24	3	-.07178	-.11511	27	1	-.12761	-.15655
24	4	-.05583	-.11511	27	2	-.11166	-.15655
24	5	-.03988	-.11511	27	3	-.09571	-.15655
24	6	-.02393	-.11511	27	4	-.07976	-.15655
24	7	-.00798	-.11511	27	5	-.06380	-.15655
24	8	.00798	-.11511	27	6	-.04785	-.15655
24	9	.02393	-.11511	27	7	-.03190	-.15655
24	10	.03988	-.11511	27	8	-.01595	-.15655
24	11	.05583	-.11511	27	9	0.00000	-.15655
24	12	.07178	-.11511	27	10	.01595	-.15655
24	13	.08773	-.11511	27	11	.03190	-.15655
24	14	.10368	-.11511	27	12	.04785	-.15655
24	15	.11963	-.11511	27	13	.06380	-.15655
24	16	.13559	-.11511	27	14	.07976	-.15655
24	17	.15154	-.11511	27	15	.09571	-.15655
24	18	.16749	-.11511	27	16	.11166	-.15655
25	1	-.09571	-.12892	28	1	-.08773	-.17037
25	2	-.07976	-.12892	28	2	-.07178	-.17037

Table 1 (Cont.)

ROW	UNIT	X	Y
28	3	-.05583	-.17037
28	4	-.03988	-.17037
28	5	-.02393	-.17037
28	6	-.00798	-.17037
28	7	.00798	-.17037
28	8	.02393	-.17037
28	9	.03988	-.17037
28	10	.05583	-.17037
28	11	.07178	-.17037
28	12	.08773	-.17037
28	13	.10368	-.17037
29	1	-.07976	-.18418
29	2	-.06380	-.18418
29	7	.01595	-.18418
29	8	.03190	-.18418
29	9	.04785	-.18418
29	10	.06380	-.18418
29	11	.07976	-.18418
30	1	.02393	-.19799
30	3	.05583	-.19799

4. SIGNAL-STRENGTH COMPUTATION

The data contained in the tables presented later can be used to estimate signal strengths for laser ranging. The signal strength can be calculated from the equation:

$$N = \frac{E}{h\nu} G_T A_S G_S A_R \frac{T^2}{R^4} \eta ,$$

where

N = number of photoelectrons,

E = transmitted energy,

h = Planck's constant,

ν = frequency of laser light.

G_T = gain of transmitter,

A_S = active reflecting area of satellite,

G_S = gain of satellite array,

A_R = area of receiving telescope,

T = atmospheric transmission factor,

R = range from station to satellite,

η = a constant that includes the quantum efficiency of the photomultiplier and the optical transmission factors of the transmitter, the satellite, and the receiver.

If the transmitted beam is a uniform spot of solid angle Ω_T , the gain function of the transmitter is

$$G_T = \frac{1}{\Omega_T} .$$

PRECEDING PAGE BLANK NOT FILMED

The active reflecting area A_g is given in Table 3 (see Section 7) as a function of the angle of incidence of the laser beam with respect to the normal to the front face of the cube corners. The gain G_g of the satellite retroreflector array is proportional to the intensity of the diffraction pattern at each point in the far field. The position of the receiver in the diffraction pattern depends on the magnitude and direction of the velocity aberration. Table 2 (Section 6) gives gain-function matrices of the array for various incidence angles and two different wavelengths.

5. METHOD OF COMPUTING TRANSFER FUNCTION

In computing gain-function matrices for the NTS-1 retroreflector array, the cube corners have been modeled as isothermal, geometrically perfect reflectors with perfect metal reflecting coatings on the back faces. The primary effect of real metal faces is a decrease in the intensity of the return signal because of the triple metallic reflection. This loss should be added to the constant η of the previous section, along with reflection losses at the front face on entering and leaving the cube corners.

The computation of the range correction includes a correction for the optical path length of the ray within the cube corner. The range correction is the difference between the centroid of the actual return signal and the centroid of the return signal that would be received from a point reflector at the center of mass of the satellite. The correction listed is the one-way correction.

The gain functions, active reflecting areas, and range corrections presented in the tables are for the incoherent case; that is, the intensities of the reflections are added without taking into account coherent interference among the reflected signals from the individual cube corners.

The variation of the range correction due to optical coherence has been derived by statistical analysis of a set of coherent returns constructed by assigning random phases to the reflection from each cube corner using a pseudo random-number generator. Since the computer time required to compute a coherent return increases as the square of the number of cube corners, the calculations were done with a reduced array obtained by replacing sets of neighboring reflectors by a single reflector at the mean position of the set. Because the coherent variations are computed from a limited number of cases, the results should be considered as only an indication of the magnitude of the effect. The incoherent range correction is the mean value of the coherent range corrections.

6. GAIN FUNCTION

Table 2 gives the gain function $G_S(\theta_1, \theta_2)$ for various angles of incidence on the array and for two wavelengths. The angles θ_1 and θ_2 are measured from the center of the return beam perpendicular and parallel, respectively, to the plane of incidence. For the particular incidence angles chosen, the gain function has the properties

$$G_S(\theta_1, \theta_2) = G_S(-\theta_1, \theta_2) = G_S(\theta_1, -\theta_2) = G_S(-\theta_1, -\theta_2) \quad .$$

Therefore, the table lists only positive values of θ_1 and θ_2 . For a collocated receiver and transmitter, the angles θ_1 and θ_2 are given by

$$\theta_1 = 2 \frac{v_1}{c} \quad , \quad \theta_2 = 2 \frac{v_2}{c} \quad ,$$

where v_1 and v_2 are the components of the transverse velocity of the satellite relative to the station perpendicular and parallel, respectively, to the plane of incidence.

For each table, the average gain function is plotted as a function of the angle from the center of the pattern, with the radius ρ given by

$$\rho = \sqrt{\theta_1^2 + \theta_2^2} \quad .$$

The direction of the illuminating laser beam is given with respect to the X, Y, Z coordinate system of the array by the two angles θ and ϕ shown in Figure 2. The angles θ_1 , θ_2 , and ρ are given in microradians in Table 2.

PRECEDING PAGE BLANK NOT FILMED

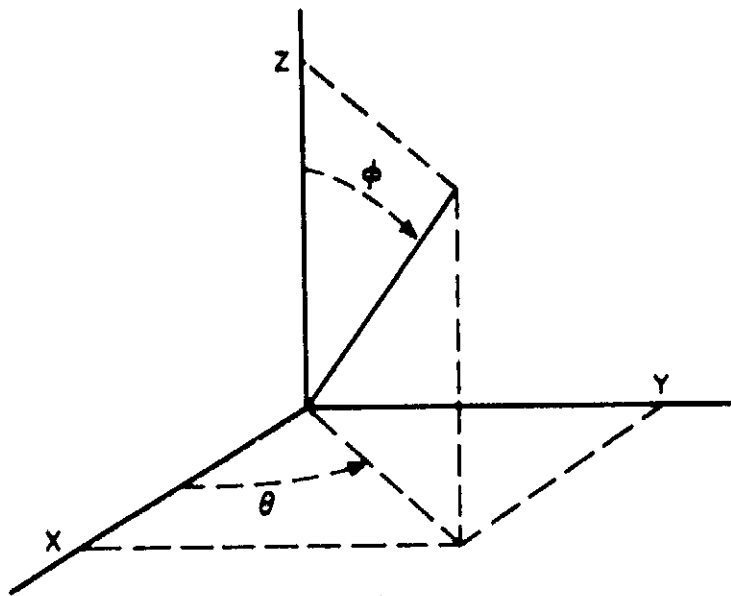


Figure 2. Coordinate system of incident beam.

Table 2. Gain-function matrices for various incidence angles and two wavelengths.

GAIN FUNCTION(1.E+7)																
θ_2	THEIA =		0		PHI =		0		WAVELENGTH		6943					
50	.17	.15	.08	.02	0.00	.05	.17	.34	.52	.64	.67					
45	1.06	.98	.76	.48	.21	.04	0.00	.09	.26	.44	.55					
40	3.04	2.88	2.41	1.77	1.08	.51	.14	0.00	.06	.22	.40					
35	6.40	6.11	5.29	4.12	2.83	1.65	.74	.20	0.00	.06	.24					
30	11.16	10.72	9.46	7.62	5.53	3.54	1.90	.77	.17	0.00	.11					
25	17.10	16.47	14.69	12.08	9.06	6.09	3.56	1.69	.56	.06	.02					
20	23.67	22.85	20.53	17.09	13.08	9.08	5.57	2.88	1.13	.24	0.00					
15	30.09	29.10	26.26	22.05	17.10	12.10	7.65	4.16	1.79	.49	.03					
10	35.52	34.37	31.12	26.27	20.53	14.70	9.46	5.30	2.41	.75	.07					
5	39.15	37.90	34.37	29.10	22.85	16.47	10.70	6.08	2.84	.94	.12					
0	40.42	39.15	35.52	30.09	23.66	17.09	11.15	6.36	3.00	1.00	.14					
	0	5	10	15	20	25	30	35	40	45	50					θ_1

p	AVERAGE GAIN FUNCTION (1.E+7)															
	0	5	10	15	20	25	30	35	40	45	50					
0	40.42															*
5	38.81															*
10	35.21														*	
15	29.86															
20	23.52														*	
25	17.03															
30	11.17														*	
35	6.43															
40	3.09														*	
45	1.10	*														
50	.20	*														

20

AVERAGE GAIN FUNCTION(1.E+7)

P	AVERAGE GRAIN LENGTH (CENTIMETERS)
0	31.17
5	30.20
10	28.01
15	24.66
20	20.55
25	16.12
30	11.81
35	7.97
40	4.86
45	2.59
50	1.13

Table 2 (Cont.)

θ_2	GAIN FUNCTION(1.E+7)										
	THEIA =	0	PHI =	20	WAVELENGTH	6943					
50	5.08	4.93	4.50	3.85	3.06	2.24	1.48	.85	.40	.12	.01
45	6.96	6.77	6.21	5.35	4.32	3.23	2.20	1.33	.68	.26	.05
40	9.08	8.83	8.13	7.06	5.76	4.37	3.05	1.91	1.02	.43	.11
35	11.34	11.05	10.20	8.91	7.32	5.62	3.98	2.55	1.42	.64	.19
30	13.66	13.31	12.32	10.79	8.92	6.91	4.95	3.23	1.85	.88	.29
25	15.90	15.51	14.37	12.63	10.49	8.17	5.91	3.90	2.28	1.12	.40
20	17.96	17.52	16.26	14.32	11.93	9.33	6.79	4.53	2.69	1.35	.51
15	19.70	19.23	17.86	15.75	13.15	10.33	7.55	5.07	3.04	1.55	.60
10	21.03	20.53	19.08	16.85	14.09	11.09	8.14	5.49	3.31	1.71	.68
5	21.86	21.34	19.84	17.53	14.67	11.56	8.50	5.75	3.49	1.81	.73
0	22.14	21.62	20.10	17.77	14.87	11.73	8.63	5.84	3.54	1.85	.74
	0	5	10	15	20	25	30	35	40	45	50 θ_1

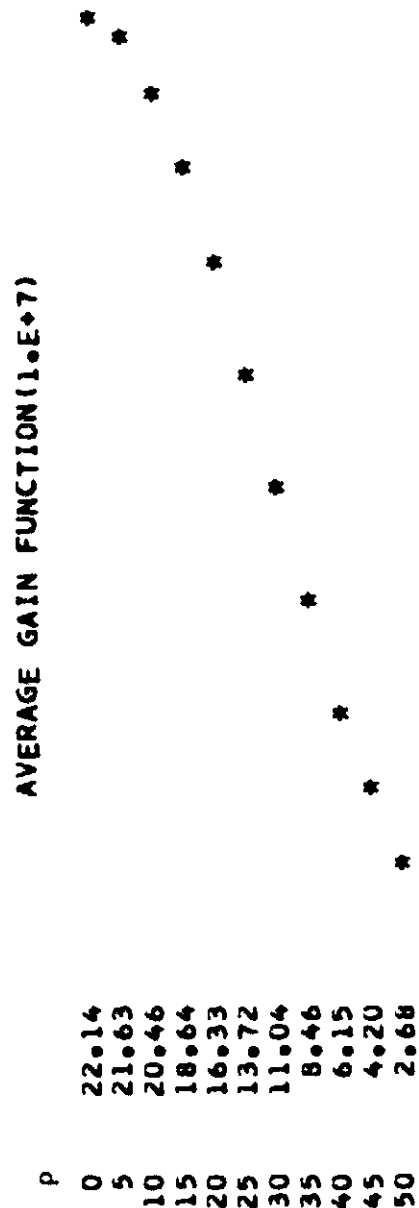


Table 2 (Cont.)

θ_2	GAIN FUNCTION(1.E+7)											θ_1
	THETA = 0		PHI = 30		WAVELENGTH 6943							
50	7.36	7.20	6.73	6.01	5.11	4.12	3.11	2.18	1.39	.78	.35	
45	8.36	8.18	7.66	6.86	5.85	4.72	3.59	2.54	1.64	.93	.43	
40	9.35	9.15	8.58	7.69	6.57	5.32	4.06	2.89	1.88	1.08	.52	
35	10.30	10.09	9.46	8.49	7.27	5.90	4.52	3.23	2.11	1.23	.60	
30	11.19	10.96	10.29	9.24	7.92	6.45	4.95	3.55	2.34	1.37	.68	
25	11.99	11.74	11.03	9.91	8.50	6.94	5.34	3.84	2.54	1.50	.75	
20	12.68	12.42	11.66	10.49	9.01	7.36	5.67	4.09	2.71	1.61	.81	
15	13.23	12.96	12.18	10.96	9.42	7.70	5.95	4.30	2.86	1.70	.86	
10	13.64	13.36	12.56	11.31	9.72	7.95	6.15	4.45	2.96	1.77	.90	
5	13.89	13.61	12.79	11.52	9.91	8.11	6.27	4.54	3.03	1.81	.92	
0	13.98	13.69	12.87	11.59	9.97	8.16	6.31	4.57	3.05	1.82	.93	
	0	5	10	15	20	25	30	35	40	45	50	θ_1

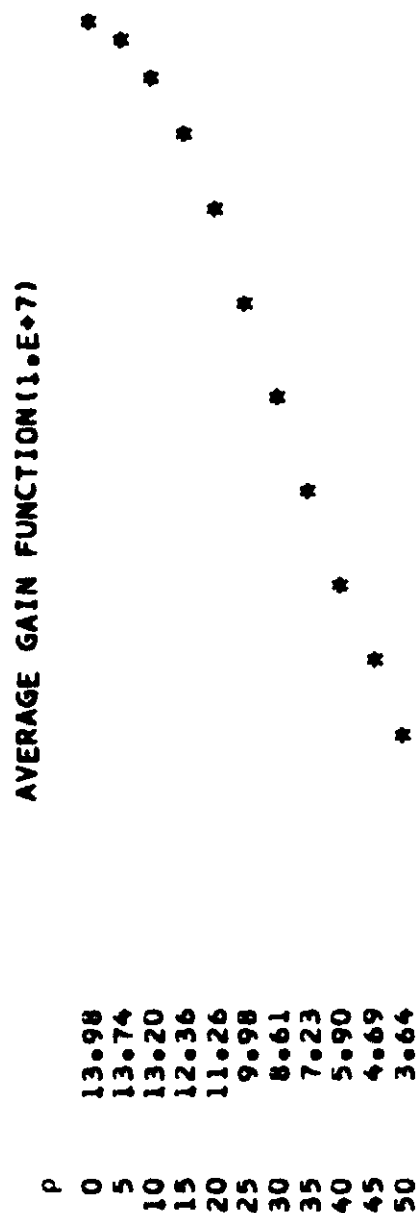


Table 2 (Cont.)

GAIN FUNCTION(1.E+7)																	
THETA = 90 PHI = 0 WAVELENGTH 6943																	
θ_2	17	15	08	02	0.00	05	17	34	52	64	67						
50	1.06	.98	.76	.48	.21	.04	0.00	.09	.26	.44	.55						
45	3.04	2.88	2.41	1.77	1.08	.51	.14	0.00	.06	.22	.40						
40	6.40	6.11	5.29	4.12	2.83	1.65	.74	.20	0.00	.06	.24						
35	11.16	10.72	9.46	7.62	5.53	3.54	1.90	.77	.17	0.00	.11						
30	17.10	16.47	14.69	12.08	9.06	6.09	3.56	1.63	.56	.06	.02						
25	23.67	22.85	20.53	17.09	13.08	9.08	5.57	2.88	1.13	.24	0.00						
20	30.09	29.10	26.26	22.05	17.10	12.10	7.65	4.16	1.79	.49	.03						
15	35.52	34.37	31.12	26.27	20.53	14.70	9.46	5.30	2.41	.75	.07						
10	39.15	37.90	34.37	29.10	22.85	16.47	10.70	6.08	2.84	.94	.12						
5	40.42	39.15	35.52	30.09	23.66	17.09	11.15	6.36	3.00	1.00	.14						
0																	
	0	5	10	15	20	25	30	35	40	45	50	θ_1					

P	AVERAGE GAIN FUNCTION(1.E+7)															
	0	5	10	15	20	25	30	35	40	45	50					
0	40.42															*
5	38.81															*
10	35.21														*	
15	29.86														*	
20	23.52														*	
25	17.03														*	
30	11.17														*	
35	6.43														*	
40	3.09														*	
45	1.10														*	
50	.20														*	

Table 2 (Cont.)

θ_2	GAIN FUNCTION(1.E+7)															
	THETA = 90								PHI = 10							
	WAVELENGTH	6943														
50	2.27	2.15	1.81	1.32	.81	.37	.09	0.00	.09	.29	.54					
45	4.23	4.04	3.49	2.69	1.81	1.01	.41	.07	.01	.14	.38					
40	6.93	6.64	5.83	4.65	3.32	2.05	1.02	.34	.03	.03	.22					
35	10.31	9.91	8.81	7.19	5.32	3.49	1.94	.83	.21	0.00	.09					
30	14.22	13.72	12.29	10.18	7.72	5.27	3.14	1.54	.53	.07	.01					
25	18.43	17.81	16.06	13.45	10.38	7.29	4.55	2.41	.99	.24	0.00					
20	22.61	21.88	19.81	16.72	13.08	9.36	6.02	3.37	1.53	.47	.05					
15	26.38	25.55	23.21	19.71	15.55	11.28	7.41	4.29	2.07	.74	.13					
10	29.38	28.49	25.93	22.10	17.54	12.84	8.55	5.06	2.54	.98	.22					
5	31.32	30.38	27.69	23.65	18.83	13.86	9.30	5.57	2.85	1.15	.29					
0	31.99	31.03	28.29	24.18	19.28	14.21	9.56	5.74	2.96	1.21	.31					

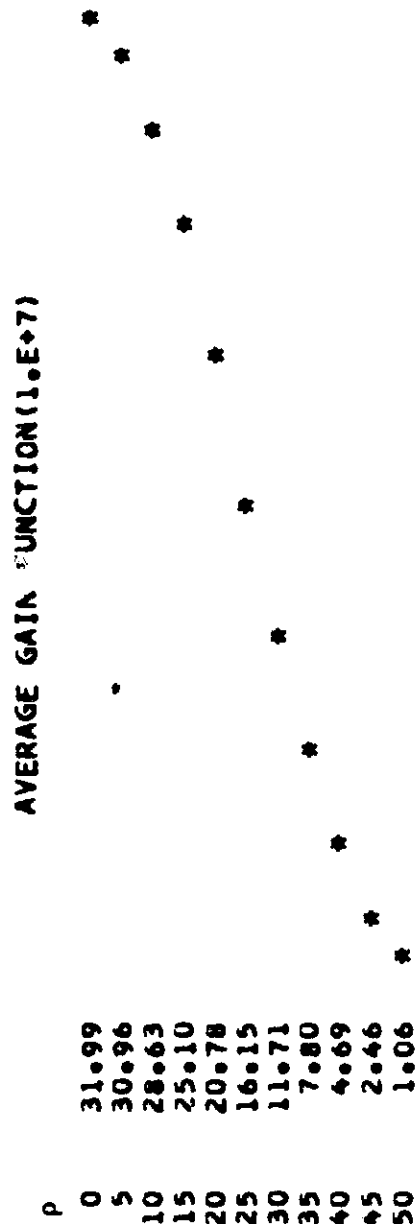


Table 2 (Cont.)

GAIN FUNCTION(1.E+7)																		
θ_2	THETA = 90								PHI = 20								WAVELENGTH 6943	θ_1
	0	5	10	15	20	25	30	35	40	45	50	55	60	65	70	75	80	
50	6.09	5.86	5.20	4.22	3.10	2.01	1.09	.44	.09	0.00	.09	.09	.09	.09	.09	.09	.09	
45	8.00	7.72	6.91	5.70	4.31	2.92	1.71	.81	.26	.02	.26	.26	.26	.26	.26	.26	.02	
40	10.12	9.78	8.81	7.37	5.68	3.97	2.46	1.28	.51	.11	.51	.51	.51	.51	.51	.51	0.00	
35	12.37	11.98	10.85	9.17	7.17	5.14	3.31	1.84	.83	.25	.83	.83	.83	.83	.83	.83	.02	
30	14.66	14.21	12.93	11.01	8.72	6.36	4.21	2.46	1.20	.44	1.20	1.20	1.20	1.20	1.20	1.20	.08	
25	16.87	16.37	14.94	12.80	10.23	7.57	5.12	3.10	1.61	.66	1.61	1.61	1.61	1.61	1.61	1.61	.17	
20	18.88	18.34	16.78	14.44	11.63	8.70	5.98	3.71	2.00	.89	2.00	2.00	2.00	2.00	2.00	2.00	.28	
15	20.59	20.01	18.35	15.84	12.83	9.67	6.72	4.24	2.36	1.10	2.36	2.36	2.36	2.36	2.36	2.36	.38	
10	21.89	21.28	19.54	16.91	13.74	10.42	7.30	4.66	2.64	1.27	2.64	2.64	2.64	2.64	2.64	2.64	.47	
5	22.71	22.08	20.29	17.58	14.32	10.89	7.66	4.92	2.82	1.38	2.82	2.82	2.82	2.82	2.82	2.82	.53	
0	22.98	22.35	20.55	17.81	14.51	11.05	7.79	5.01	2.88	1.42	2.88	2.88	2.88	2.88	2.88	2.88	.55	

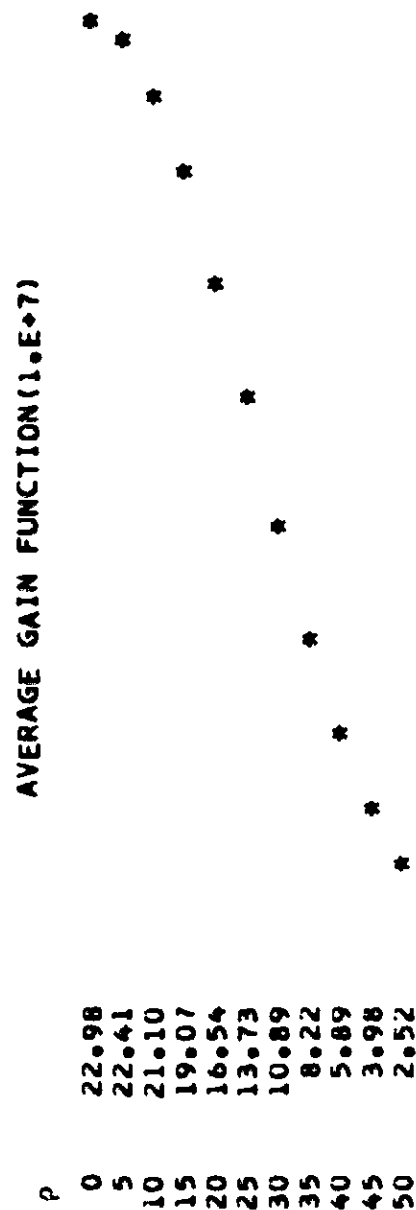


Table 2 (Cont.)

GAIN FUNCTION(1.E+7)															
θ_2	THETA = 90					PHI = 30					WAVELENGTH 6943				
	0	5	10	15	20	25	30	35	40	45	50	θ_1			
50	7.66	7.46	6.87	5.98	4.90	3.75	2.66	1.71	.98	.47	.17				
45	8.63	8.41	7.77	6.80	5.61	4.35	3.14	2.08	1.24	.64	.26				
40	9.59	9.35	8.66	7.61	6.33	4.95	3.62	2.45	1.50	.81	.37				
35	10.51	10.25	9.52	8.40	7.02	5.54	4.10	2.82	1.77	1.00	.48				
30	11.37	11.10	10.32	9.13	7.67	6.09	4.55	3.17	2.04	1.18	.60				
25	12.14	11.86	11.05	9.80	8.26	6.60	4.97	3.50	2.28	1.36	.72				
20	12.81	12.52	11.68	10.38	8.78	7.04	5.33	3.79	2.50	1.51	.82				
15	13.36	13.06	12.19	10.85	9.20	7.40	5.63	4.02	2.68	1.64	.91				
10	13.76	13.45	12.56	11.20	9.51	7.67	5.85	4.20	2.81	1.74	.98				
5	14.01	13.69	12.79	11.41	9.69	7.83	5.98	4.31	2.90	1.80	1.02				
0	14.09	13.77	12.87	11.48	9.76	7.88	6.03	4.34	2.92	1.82	1.03				

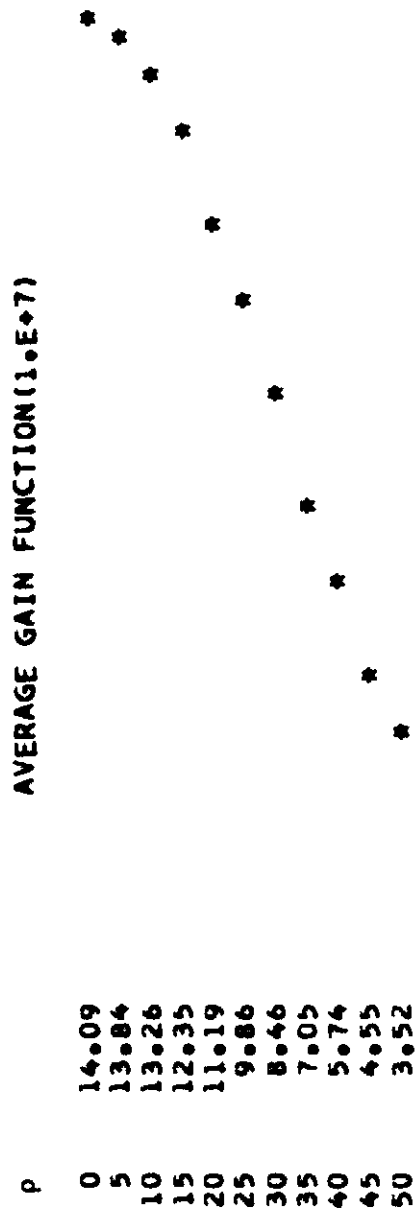


Table 2 (Cont.)

θ_2	GAIN FUNCTION(1.E+7)										
	THETA =	0	PHI =	0	WAVELENGTH	5300					
50	.72	.77	.91	1.12	1.34	1.48	1.45	1.22	.82	.40	.09
45	.23	.27	.41	.65	.97	1.27	1.44	1.37	1.05	.61	.21
40	.04	.02	0.00	.08	.32	.69	1.05	1.23	1.13	.79	.37
35	1.44	1.24	.76	.26	.01	.11	.47	.85	1.02	.88	.54
30	5.88	5.35	3.97	2.27	.86	.11	.04	.39	.77	.89	.71
25	14.37	13.33	10.55	6.95	3.57	1.21	.13	.06	.46	.81	.85
20	26.76	25.06	20.47	14.33	8.28	3.62	.93	.03	.20	.69	.96
15	41.41	38.98	32.40	23.45	14.37	7.02	2.36	.30	.05	.56	1.03
10	55.46	52.38	43.95	32.41	20.49	10.59	4.00	.77	0.00	.46	1.08
5	65.65	62.09	52.38	38.99	25.06	13.31	5.30	1.18	.01	.39	1.10
0	69.37	65.65	55.46	41.41	26.74	14.33	5.80	1.35	.02	.37	1.11
	0	5	10	15	20	25	30	35	40	45	50 θ_1

AVERAGE GAIN FUNCTION(1.E+7)

P	0	5	10	15	20	25	30	35	40	45	50
0	69.37										*
5	64.69									*	
10	54.69								*		
15	40.95						*				
20	26.63				*						
25	14.45			*							
30	6.05		*								
35	1.58	*									
40	.15	*									
45	.33	*									
50	.88	*									

Table 2 (Cont.)

GAIN FUNCTION(1.E+7)												
θ_2	THETA = 0			PHI = 10			WAVELENGTH 5300					
	0	5	10	15	20	25	30	35	40	45	50	θ_1
50	0.00	.01	.04	.13	.29	.50	.70	.81	.78	.60	.35	
45	.35	.30	.16	.03	.01	.13	.35	.57	.68	.63	.44	
40	2.00	1.81	1.32	.72	.24	.01	.06	.28	.50	.60	.52	
35	5.55	5.15	4.08	2.68	1.36	.44	.03	.06	.30	.52	.58	
30	11.31	10.61	8.73	6.19	3.63	1.61	.41	.01	.13	.42	.62	
25	19.14	18.08	15.18	11.19	7.04	3.57	1.27	.18	.02	.31	.64	
20	28.35	26.88	22.86	17.24	11.28	6.14	2.51	.58	0.00	.21	.64	
15	37.76	35.90	30.76	23.53	15.78	8.94	3.96	1.11	.06	.14	.63	
10	45.94	43.74	37.65	29.06	19.77	11.47	5.30	1.64	.16	.09	.62	
5	51.51	49.09	42.37	32.86	22.53	13.24	6.26	2.03	.24	.07	.61	
0	53.49	50.98	44.05	34.21	23.52	13.87	6.61	2.18	.27	.06	.61	

p	AVERAGE GAIN FUNCTION(1.E+7)										
	0	5	10	15	20	25	30	35	40	45	50
0	53.49										*
5	50.66									*	
10	44.49								*		
15	35.64							*			
20	25.77					*					
25	16.49			*							
30	9.05		*								
35	3.97	*									
40	1.21	*									
45	.20	*									
50	.21	*									

Table 2 (Cont.)

θ_2	GAIN FUNCTION (1.E+7)											θ_1
	THETA = 0	PHI = 20	WAVELENGTH 5300									
50	2.03	1.89	1.51	1.01	.52	.17	.01	.03	.14	.26	.32	
45	4.21	3.96	3.29	2.37	1.43	.65	.18	0.00	.05	.20	.32	
40	7.34	6.95	5.90	4.43	2.86	1.51	.57	.10	.01	.13	.31	
35	11.37	10.82	9.30	7.15	4.82	2.73	1.20	.32	.01	.08	.29	
30	16.11	15.38	13.33	10.42	7.21	4.28	2.04	.66	.07	.04	.27	
25	21.26	20.33	17.73	14.01	9.88	6.04	3.03	1.09	.17	.01	.25	
20	26.39	25.27	22.14	17.63	12.58	7.85	4.07	1.57	.31	0.00	.22	
15	31.05	29.76	26.15	20.93	15.07	9.53	5.06	2.04	.46	0.00	.21	
10	34.77	33.34	29.36	23.58	17.07	10.89	5.86	2.43	.58	.01	.19	
5	37.17	35.66	31.43	25.30	18.37	11.78	6.39	2.68	.67	.01	.18	
0	38.00	36.46	32.15	25.89	18.82	12.08	6.58	2.78	.70	.02	.18	

P	AVERAGE GAIN FUNCTION (1.E+7)										
	0	5	10	15	20	25	30	35	40	45	50
0	38.00									*	
5	36.50									*	
10	33.17								*		
15	28.22							*			
20	22.39						*				
25	16.44					*					
30	11.08			*							
35	6.73		*								
40	3.63	*									
45	1.70	*									
50	.71	*									

Table 2 (Cont.)

θ_2	GAIN FUNCTION(1.E+7)															
	THEIA = 0		PHI = 30		WAVELENGTH 5300											
50	7.53	7.24	6.40	5.17	3.78	2.43	1.32	.55	.13	0.00	.06					
45	8.60	9.23	8.19	6.67	4.93	3.24	1.81	.80	.22	.01	.05					
40	11.80	11.36	10.11	8.28	6.18	4.11	2.36	1.08	.33	.02	.04					
35	14.06	13.54	12.09	9.95	7.47	5.02	2.93	1.38	.45	.05	.03					
30	16.28	15.70	14.04	11.59	8.75	5.93	3.51	1.70	.57	.07	.02					
25	18.38	17.73	15.88	13.15	9.97	6.80	4.06	2.00	.70	.10	.01					
20	20.26	19.55	17.53	14.54	11.06	7.58	4.56	2.27	.82	.13	.01					
15	21.83	21.07	18.91	15.71	11.97	8.24	4.98	2.50	.92	.16	.01					
10	23.01	22.21	19.94	16.58	12.66	8.74	5.30	2.68	1.00	.18	.01					
5	23.74	22.92	20.59	17.13	13.09	9.05	5.50	2.79	1.04	.19	0.00					
0	23.99	23.16	20.80	17.32	13.24	9.15	5.57	2.83	1.06	.19	0.00					

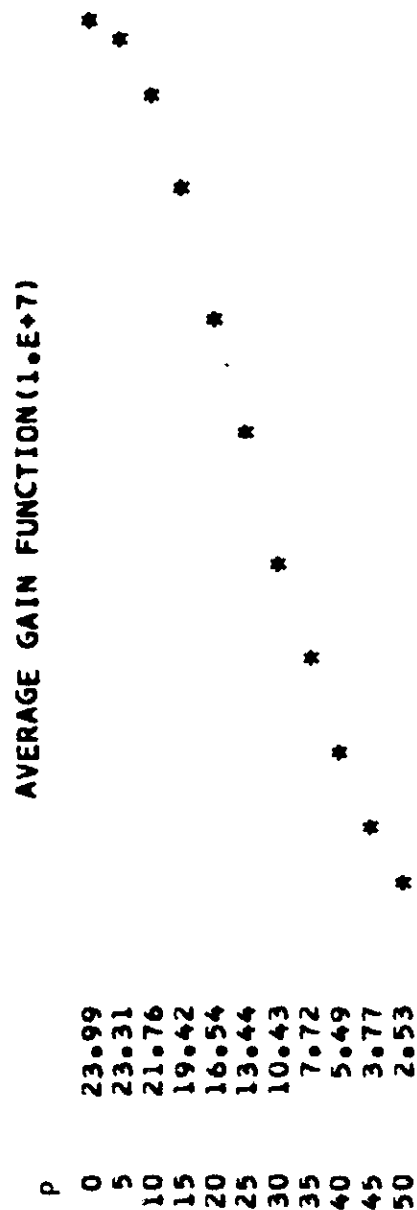


Table 2 (Cont.)

θ_2	GAIN FUNCTION(1.E+7)															
	THEIA = 90								PHI = 0							
	WAVELENGTH 5300															
	0	5	10	15	20	25	30	35	40	45	50	θ_1				
50	.72	.77	.91	1.12	1.34	1.48	1.45	1.22	.82	.40	.09					
45	.23	.27	.41	.65	.97	1.27	1.44	1.37	1.05	.61	.21					
40	.04	.02	0.00	.08	.32	.69	1.05	1.23	1.13	.79	.37					
35	1.44	1.24	.76	.26	.01	.11	.47	.85	1.02	.88	.54					
30	5.88	5.35	3.97	2.27	.86	.11	.04	.39	.77	.89	.71					
25	14.37	13.33	10.55	6.95	3.57	1.21	.13	.06	.46	.81	.85					
20	26.76	25.06	20.47	14.33	8.28	3.62	.93	.03	.20	.69	.96					
15	41.41	38.98	32.40	23.45	14.37	7.02	2.36	.30	.05	.56	1.03					
10	55.46	52.38	43.95	32.41	20.49	10.59	4.00	.77	0.00	.46	1.08					
5	65.65	62.09	52.38	38.49	25.06	13.31	5.30	1.18	.01	.39	1.10					
0	69.37	65.65	55.46	41.41	26.74	14.33	5.80	1.35	.02	.37	1.11					

AVERAGE GAIN FUNCTION(1.E+7)

P	0	5	10	15	20	25	30	35	40	45	50
0	69.37										*
5	64.69									*	
10	54.69								*		
15	40.95						*				
20	26.63					*					
25	14.45			*							
30	6.05		*								
35	1.58	*									
40	.15	*									
45	.33	*									
50	.88	*									

Table 2 (Cont.)

		GAIN FUNCTION(1.E+7)														
θ_2		THETA = 90		PHI = 10		WAVELENGTH 5300										
50		.03	.02	0.00	.05	.21	.49	.83	1.11	1.25	1.18	.94				
45		.70	.59	.34	.09	0.00	.17	.55	1.00	1.33	1.41	1.23				
40		2.72	2.44	1.73	.88	.23	0.00	.22	.71	1.20	1.46	1.40				
35		6.61	6.07	4.66	2.86	1.24	.25	.01	.34	.90	1.32	1.40				
30		12.63	11.75	9.40	6.30	3.32	1.16	.13	.07	.54	1.05	1.27				
25		20.62	19.33	15.86	11.17	6.49	2.84	.71	.01	.23	.73	1.05				
20		29.88	28.16	23.47	17.06	10.51	5.17	1.74	.22	.04	.44	.80				
15		39.28	37.14	31.28	23.21	14.83	7.80	3.05	.65	0.00	.23	.58				
10		47.41	44.92	38.09	28.63	18.71	10.24	4.34	1.16	.07	.11	.42				
5		52.94	50.22	42.75	32.36	21.41	11.97	5.29	1.56	.15	.05	.33				
0		54.90	52.10	44.40	33.69	22.38	12.60	5.64	1.72	.19	.03	.30				
		0	5	10	15	20	25	30	35	40	45	50	θ_1			

AVERAGE GAIN FUNCTION(1.E+7)

P																	
0	54.90																*
5	51.90																*
10	45.36																*
15	36.05																*
20	25.78																*
25	16.25																*
30	8.75																*
35	3.76																*
40	1.14																*
45	.25																*
50	.29																*

Table 2 (Cont.)

GAIN FUNCTION(1.E+7)

θ_2	THETA = 90										PHI = 20										WAVELENGTH 5300																				θ_1
	0	5	10	15	20	25	30	35	40	45	50	0	5	10	15	20	25	30	35	40	45	50	0	5	10	15	20	25	30	35	40	45	50								
50	3.28	2.98	2.21	1.24	.44	.03	.08	.47	.94	1.26	1.30	3.28	2.98	2.21	1.24	.44	.03	.08	.47	.94	1.26	1.30	5.73	5.29	4.11	2.60	1.20	.29	0.00	.21	.65	1.04	1.18								
45	5.73	5.29	4.11	2.60	1.20	.29	0.00	.21	.65	1.04	1.18	9.03	8.42	6.77	4.58	2.45	.89	.11	.04	.38	.77	.98	9.03	8.42	6.77	4.58	2.45	.89	.11	.04	.38	.77	.98								
40	9.03	8.42	6.77	4.58	2.45	.89	.11	.04	.38	.77	.98	13.15	12.34	10.15	7.18	4.21	1.86	.47	.01	.15	.51	.76	13.15	12.34	10.15	7.18	4.21	1.86	.47	.01	.15	.51	.76								
35	13.15	12.34	10.15	7.18	4.21	1.86	.47	.01	.15	.51	.76	17.90	16.88	14.11	10.31	6.40	3.18	1.09	.14	.02	.28	.54	17.90	16.88	14.11	10.31	6.40	3.18	1.09	.14	.02	.28	.54								
30	17.90	16.88	14.11	10.31	6.40	3.18	1.09	.14	.02	.28	.54	23.00	21.77	18.41	13.76	8.90	4.77	1.92	.44	.01	.12	.35	23.00	21.77	18.41	13.76	8.90	4.77	1.92	.44	.01	.12	.35								
25	23.00	21.77	18.41	13.76	8.90	4.77	1.92	.44	.01	.12	.35	28.06	26.63	22.72	17.26	11.48	6.46	2.88	.86	.08	.03	.21	28.06	26.63	22.72	17.26	11.48	6.46	2.88	.86	.08	.03	.21								
20	28.06	26.63	22.72	17.26	11.48	6.46	2.88	.86	.08	.03	.21	32.63	31.03	26.63	20.47	13.88	8.08	3.83	1.31	.22	0.00	.12	32.63	31.03	26.63	20.47	13.88	8.08	3.83	1.31	.22	0.00	.12								
15	32.63	31.03	26.63	20.47	13.88	8.08	3.83	1.31	.22	0.00	.12	36.27	34.54	29.77	23.06	15.84	9.42	4.65	1.73	.37	.01	.06	36.27	34.54	29.77	23.06	15.84	9.42	4.65	1.73	.37	.01	.06								
10	36.27	34.54	29.77	23.06	15.84	9.42	4.65	1.73	.37	.01	.06	38.63	36.81	31.80	24.74	17.12	10.31	5.19	2.02	.49	.02	.04	38.63	36.81	31.80	24.74	17.12	10.31	5.19	2.02	.49	.02	.04								
5	38.63	36.81	31.80	24.74	17.12	10.31	5.19	2.02	.49	.02	.04	39.44	37.60	32.50	25.32	17.56	10.62	5.39	2.12	.53	.03	.03	39.44	37.60	32.50	25.32	17.56	10.62	5.39	2.12	.53	.03	.03								
0	39.44	37.60	32.50	25.32	17.56	10.62	5.39	2.12	.53	.03	.03																														

AVERAGE GAIN FUNCTION(1.E+7)

P	0	5	10	15	20	25	30	35	40	45	50
0	39.44										
5	37.76										
10	34.05										
15	28.61										
20	22.33										
25	16.09										
30	10.64										
35	6.37										
40	3.43										
45	1.65										
50	.76										

Table 2 (Cont.)

θ_2	GAIN FUNCTION(1.E+7)											θ_1
	THETA = 90			PHI = 30			WAVELENGTH 5300					
50	8.28	7.85	6.66	5.00	3.24	1.73	.67	.13	0.00	.11	.28	
45	10.25	9.75	8.37	6.41	4.32	2.46	1.10	.32	.02	.03	.16	
40	12.36	11.79	10.20	7.96	5.51	3.30	1.62	.58	.10	0.00	.08	
35	14.53	13.89	12.11	9.57	6.78	4.22	2.22	.91	.24	.01	.02	
30	16.68	15.97	14.01	11.19	8.07	5.16	2.85	1.28	.41	.06	0.00	
25	18.71	17.94	15.81	12.74	9.31	6.09	3.48	1.67	.61	.14	0.00	
20	20.53	19.72	17.44	14.14	10.45	6.95	4.08	2.04	.82	.23	.03	
15	22.06	21.20	18.80	15.32	11.41	7.68	4.59	2.37	1.01	.32	.06	
10	23.22	22.32	19.83	16.22	12.14	8.24	4.99	2.63	1.16	.40	.09	
5	23.93	23.02	20.47	16.78	12.60	8.59	5.24	2.80	1.26	.45	.11	
0	24.18	23.26	20.69	16.97	12.75	8.71	5.33	2.86	1.29	.46	.11	
	0	5	10	15	20	25	30	35	40	45	50	θ_1

AVERAGE GAIN FUNCTION(1.E+7)

p	0	5	10	15	20	25	30	35	40	45	50
0	24.18										*
5	23.44									*	
10	21.79								*		
15	19.31									*	
20	16.32							*			
25	13.16					*					
30	10.15				*						
35	7.48			*							
40	5.31		*								
45	3.63	*									
50	2.42	*									

7. ACTIVE REFLECTING AREA

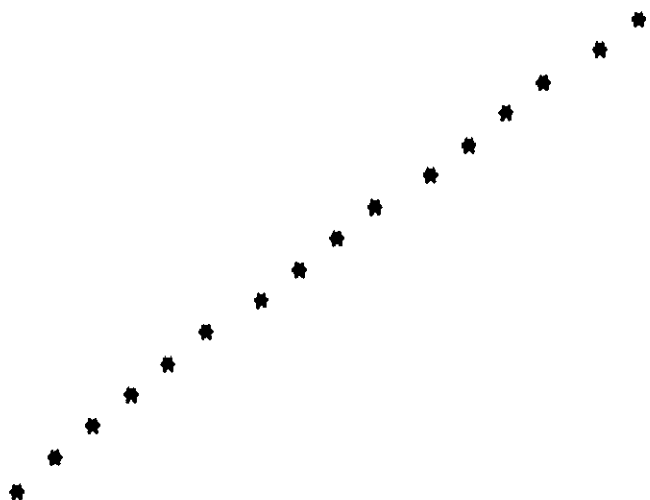
The active reflecting area is a function of the two incidence angles θ and ϕ giving the direction of the incident beam, as drawn in Figure 2. We note there is only a slight variation with the angle θ . Table 3 shows the active reflecting area as a function of ϕ for two azimuths, representing the maximum and minimum area. The effective reflecting area in the table is in units of the equivalent number of cube corners at normal incidence. The implied axes of the computer graph are such that the incidence angle increases down the page and the active reflecting area increases to the right.

Table 3. Active reflecting area as a function of angle of incidence.

a) $\theta = 0$

PHI(DEG) EFFECTIVE REFLECTING AREA

0.0	420.0000
2.0	400.9155
4.0	381.7007
6.0	362.4139
8.0	343.1123
10.0	323.8524
12.0	304.6894
14.0	285.6778
16.0	266.8711
18.0	248.3218
20.0	230.0814
22.0	212.2001
24.0	194.7269
26.0	177.7098
28.0	161.1948
30.0	145.2265

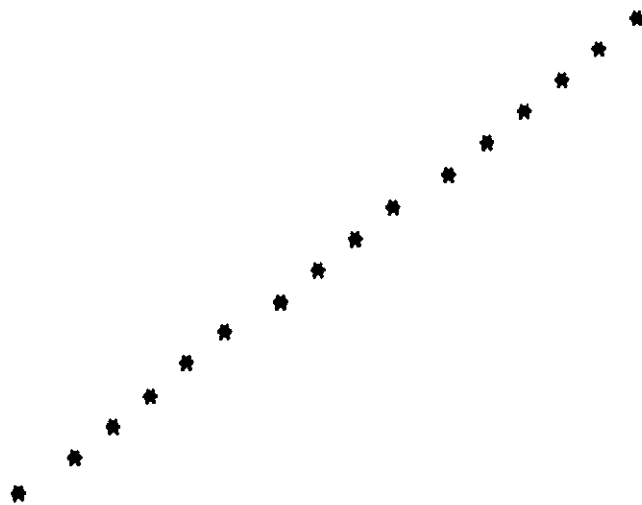


ONE REFLECTOR AT NORMAL INCIDENCE HAS A REFLECTING AREA OF UNITY

b) $\theta = 90$

PHI(DEG) EFFECTIVE REFLECTING AREA

0.0	420.0000
2.0	403.2985
4.0	386.1375
6.0	368.5696
8.0	350.6484
10.0	332.4283
12.0	313.9644
14.0	295.3126
16.0	276.5300
18.0	257.6745
20.0	238.8050
22.0	219.9814
24.0	201.2647
26.0	182.7169
28.0	164.4010
30.0	146.3809



ONE REFLECTOR AT NORMAL INCIDENCE HAS A REFLECTING AREA OF UNITY

8. RANGE CORRECTION

The range correction that must be added to a laser range measurement to obtain the range to the center of mass of the satellite is given in Table 4. The values are for the incoherent case, which is the mean of the coherent cases. The correction is listed as a function of the angle between the incident beam and the symmetry axis (Z axis) of the satellite. In the computer graph, the range correction is plotted to the right at 1 cm per print position, and the incidence angle is down the page. The range correction that includes the effect of optical path length in the cube corner is given by

$$\text{Range correction} = Z \cos \phi - L \sqrt{n^2 - \sin^2 \phi},$$

where

Z = distance from the center of mass to the front face of the retroreflectors
(0.34544 m),

ϕ = the angle between the incident beam and the Z axis of the satellite,

L = the length of the cube corner from vertex to face ($0.015/\sqrt{2} = 0.0106$ m),

n = the index of refraction of fused silica (1.455).

Table 4. Range correction.

PHI (DEG)	RANGE CORRECTION (METERS)
0.0	.3300
2.0	.3298
4.0	.3292
6.0	.3282
8.0	.3267
10.0	.3249
12.0	.3226
14.0	.3200
16.0	.3169
18.0	.3135
20.0	.3096
22.0	.3054
24.0	.3008
26.0	.2958
28.0	.2904
30.0	.2847

*
*
*
*
*
*
*
*
*
*
*
*
*
*
*
*
*
*
*
*

9. PULSE SPREADING

Except at normal incidence, the reflected pulse from the array will be wider, on the average, than the transmitted pulse because the cube corners are not all at the same distance from the observer. The effect is negligible except for very short pulses, such as those from mode-locked lasers. One measure of the effect is the distance of the half-power point on the leading edge from the pulse centroid. Table 5 lists the increase of this quantity for the incoherent case for three different incident-pulse lengths. The values shown are the one-way range error that would result in a half-maximum detection system. Tests made with large numbers of coherent returns do not indicate that the incoherent-pulse spreading at the half-power point is the mean of the spreading for the coherent pulses. The use of Table 5 to correct range data for pulse spreading would, therefore, be questionable.

PRECEDING PAGE BLANK NOT FILMED

Table 5. Pulse spread.

20 NANOSECOND PULSE THETA = 90		5 NANOSECOND PULSE THETA = 90	
PHI(DEG)	PULSE SPREADING(METERS)	PHI(DEG)	PULSE SPREADING(METERS)
0.0	0.0000 *	0.0	0.0000 *
2.0	0.0000 *	2.0	0.0000 *
4.0	0.0000 *	4.0	.0001 *
6.0	.0001 *	6.0	.0002 *
8.0	.0001 *	8.0	.0004 *
10.0	.0001 *	10.0	.0006 *
12.0	.0002 *	12.0	.0009 *
14.0	.0003 *	14.0	.0012 *
16.0	.0004 *	16.0	.0016 *
18.0	.0005 *	18.0	.0020 *
20.0	.0006 *	20.0	.0025 *
22.0	.0007 *	22.0	.0030 *
24.0	.0009 *	24.0	.0035 *
26.0	.0010 *	26.0	.0041 *
28.0	.0012 *	28.0	.0047 *
30.0	.0013 *	30.0	.0053 *

.2 NANOSECOND PULSE THETA = 90

PHI(DEG) PULSE SPREADING(METERS)

0.0	-0.0000 *
2.0	.0007 *
4.0	.0027 *
6.0	.0065 *
8.0	.0116 *
10.0	.0173 *
12.0	.0230 *
14.0	.0286 *
16.0	.0341 *
18.0	.0396 *
20.0	.0451 *
22.0	.0504 *
24.0	.0558 *
26.0	.0610 *
28.0	.0662 *
30.0	.0713 *

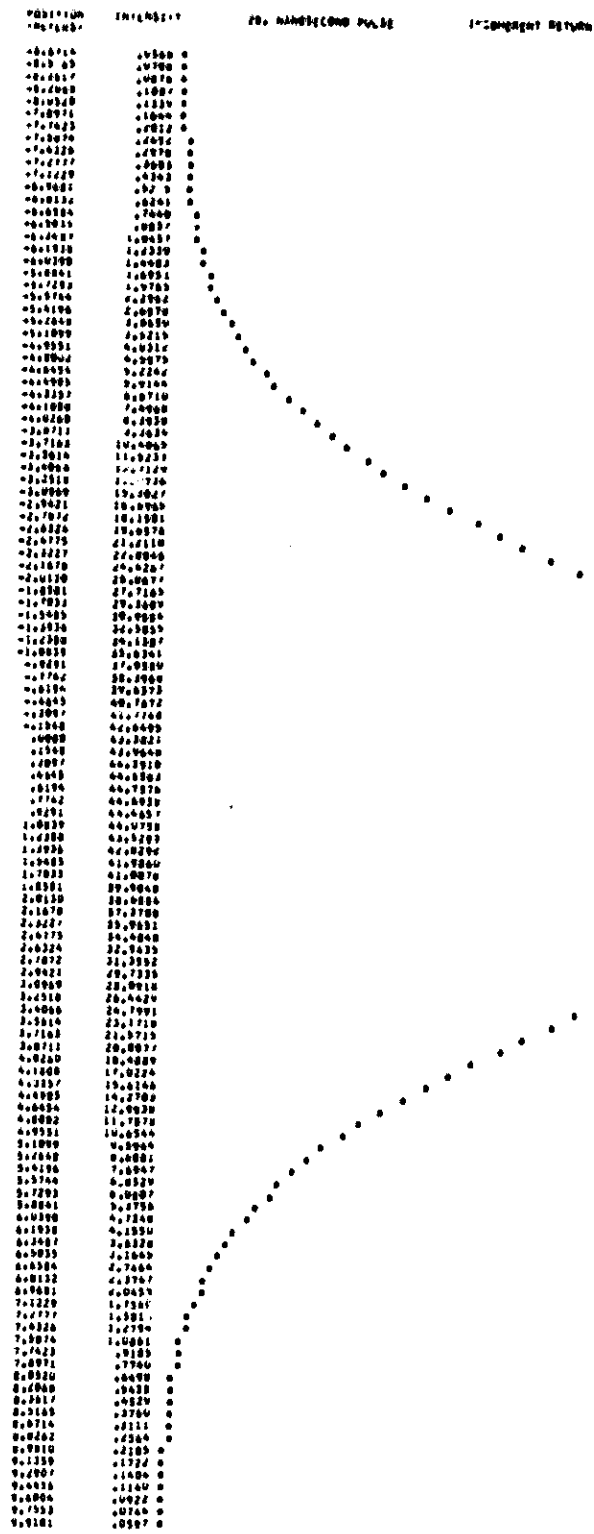
10. VARIATIONS IN PULSE SHAPE DUE TO OPTICAL COHERENCE

Since the transmitted laser pulse is coherent, the reflections from individual cube corners will interfere with each other. For long pulses, the effect is primarily on the amplitude and centroid of the return pulse, with the shape remaining nearly the same as that of the incident pulse. When the pulse length is on the order of the spread in range to the individual cube corners, both the shape and the size of the reflected pulse vary. Figure 3 shows examples of coherent returns from the array at a 15° incidence angle. The incoherent return at this angle has a strength equivalent to 285.9 cube corners, and the centroid of the pulse is at 0.6370 m. The strength and centroid for the pulses shown is given in Table 6. The position (in meters) and the intensity (in normalized units) are listed beside each curve of Figure 3. The intensity is in units such that the area under the curve is equal to the signal strength in equivalent number of cube corners. Position is measured toward the observer, with the origin at the center of the pulse that would be received from a point reflector at the satellite center of mass.

Table 6. Pulse strength and centroid.

$$\theta = 90^\circ, \phi = 15^\circ$$

Pulse width (nsec)	Type of return	Centroid (m)	Signal strength	Figure
20	Incoherent	0.6370	285.9341	3a
20	Coherent	0.7249	238.1188	3b
5	Incoherent	0.6370	285.9341	3c
5	Coherent	0.6693	647.5280	3d
0.2	Incoherent	0.6370	285.9341	3e
0.2	Coherent	0.6376	223.7706	3f
0.2	Coherent	0.6462	119.0431	3g
0.2	Coherent	0.6987	376.0539	3h
0.2	Coherent	0.6447	158.3388	3i
0.2	Coherent	0.6087	206.7810	3j



REPRODUCIBILITY OF THE
ORIGINAL PAGE IS POOR

Figure 3a. Coherent pulse shapes.

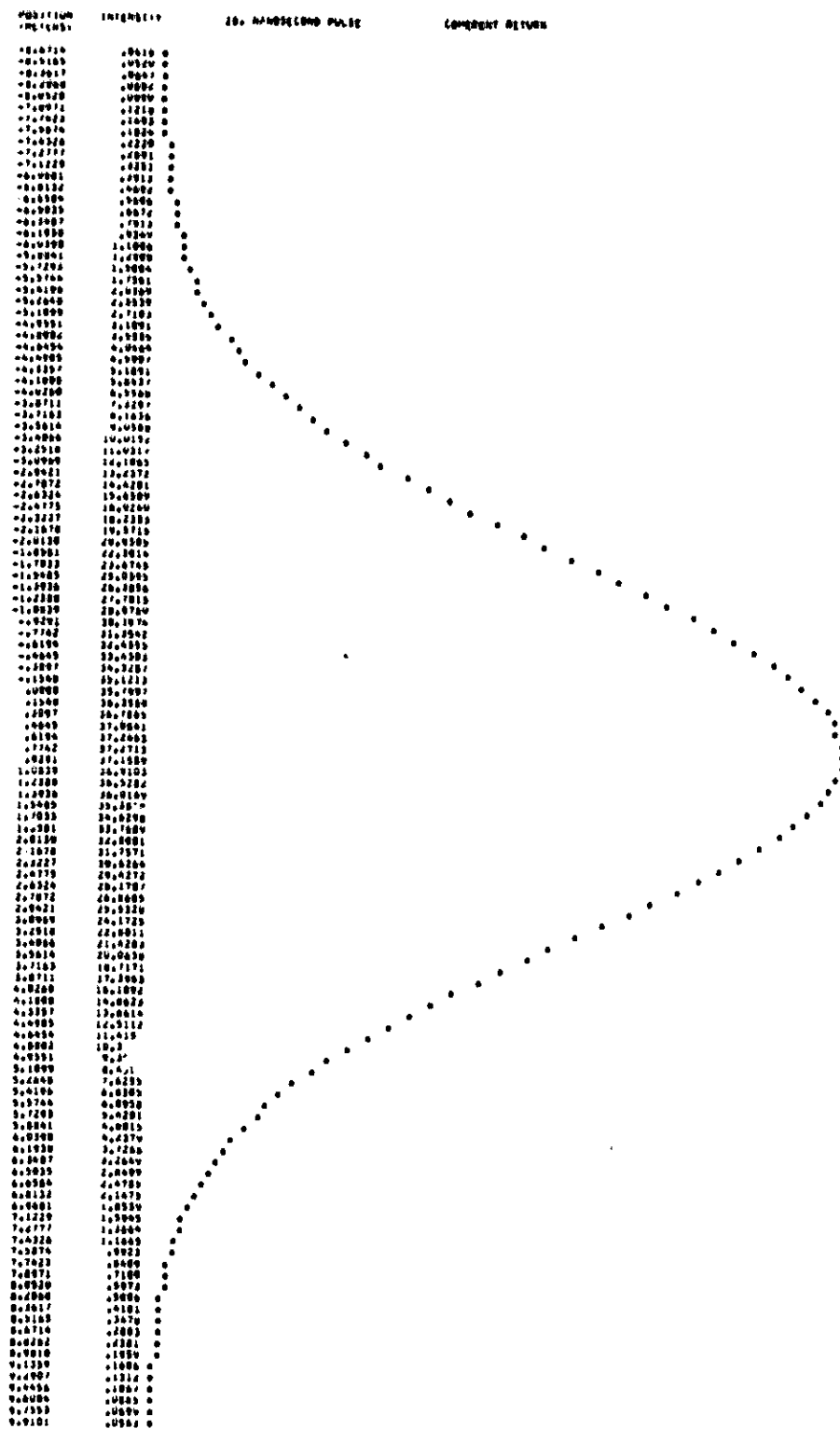
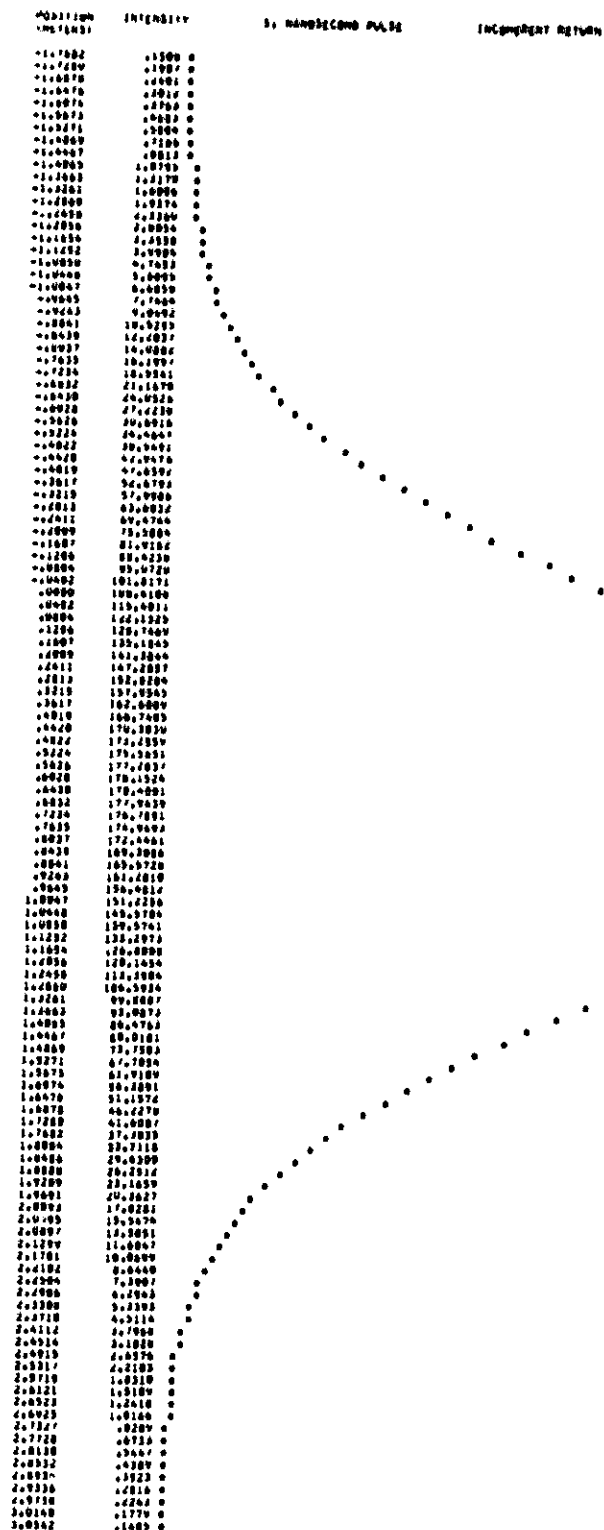


Figure 3b.



REPRODUCIBILITY OF THE
ORIGINAL PAGE IS POOR

Figure 3c.

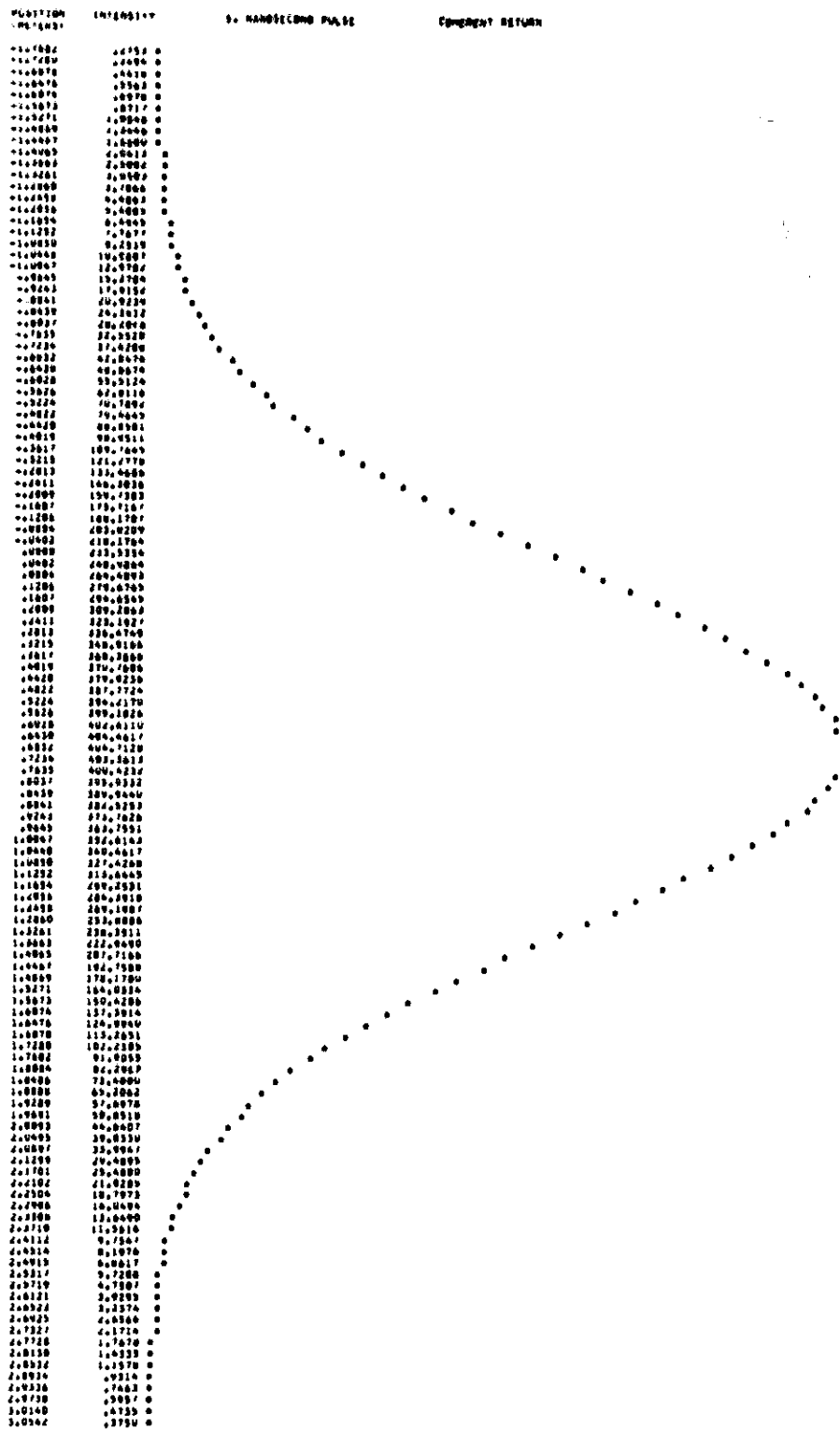


Figure 3d.

PULSE NUMBER	INTERLACE	2 HANDS (COND. PULSE)	CONVERTER RETURN
00000	00000	0	0
00001	00001	0	0
00002	00002	0	0
00003	00003	0	0
00004	00004	0	0
00005	00005	0	0
00006	00006	0	0
00007	00007	0	0
00008	00008	0	0
00009	00009	0	0
00010	00010	0	0
00011	00011	0	0
00012	00012	0	0
00013	00013	0	0
00014	00014	0	0
00015	00015	0	0
00016	00016	0	0
00017	00017	0	0
00018	00018	0	0
00019	00019	0	0
00020	00020	0	0
00021	00021	0	0
00022	00022	0	0
00023	00023	0	0
00024	00024	0	0
00025	00025	0	0
00026	00026	0	0
00027	00027	0	0
00028	00028	0	0
00029	00029	0	0
00030	00030	0	0
00031	00031	0	0
00032	00032	0	0
00033	00033	0	0
00034	00034	0	0
00035	00035	0	0
00036	00036	0	0
00037	00037	0	0
00038	00038	0	0
00039	00039	0	0
00040	00040	0	0
00041	00041	0	0
00042	00042	0	0
00043	00043	0	0
00044	00044	0	0
00045	00045	0	0
00046	00046	0	0
00047	00047	0	0
00048	00048	0	0
00049	00049	0	0
00050	00050	0	0
00051	00051	0	0
00052	00052	0	0
00053	00053	0	0
00054	00054	0	0
00055	00055	0	0
00056	00056	0	0
00057	00057	0	0
00058	00058	0	0
00059	00059	0	0
00060	00060	0	0
00061	00061	0	0
00062	00062	0	0
00063	00063	0	0
00064	00064	0	0
00065	00065	0	0
00066	00066	0	0
00067	00067	0	0
00068	00068	0	0
00069	00069	0	0
00070	00070	0	0
00071	00071	0	0
00072	00072	0	0
00073	00073	0	0
00074	00074	0	0
00075	00075	0	0
00076	00076	0	0
00077	00077	0	0
00078	00078	0	0
00079	00079	0	0
00080	00080	0	0
00081	00081	0	0
00082	00082	0	0
00083	00083	0	0
00084	00084	0	0
00085	00085	0	0
00086	00086	0	0
00087	00087	0	0
00088	00088	0	0
00089	00089	0	0
00090	00090	0	0
00091	00091	0	0
00092	00092	0	0
00093	00093	0	0
00094	00094	0	0
00095	00095	0	0
00096	00096	0	0
00097	00097	0	0
00098	00098	0	0
00099	00099	0	0
00100	00100	0	0
00101	00101	0	0
00102	00102	0	0
00103	00103	0	0
00104	00104	0	0
00105	00105	0	0
00106	00106	0	0
00107	00107	0	0
00108	00108	0	0
00109	00109	0	0
00110	00110	0	0
00111	00111	0	0
00112	00112	0	0
00113	00113	0	0
00114	00114	0	0
00115	00115	0	0
00116	00116	0	0
00117	00117	0	0
00118	00118	0	0
00119	00119	0	0
00120	00120	0	0
00121	00121	0	0
00122	00122	0	0
00123	00123	0	0
00124	00124	0	0
00125	00125	0	0
00126	00126	0	0
00127	00127	0	0
00128	00128	0	0
00129	00129	0	0
00130	00130	0	0
00131	00131	0	0
00132	00132	0	0
00133	00133	0	0
00134	00134	0	0
00135	00135	0	0
00136	00136	0	0
00137	00137	0	0
00138	00138	0	0
00139	00139	0	0
00140	00140	0	0
00141	00141	0	0
00142	00142	0	0
00143	00143	0	0
00144	00144	0	0
00145	00145	0	0
00146	00146	0	0
00147	00147	0	0
00148	00148	0	0
00149	00149	0	0
00150	00150	0	0

Figure 3f.

REPRODUCIBILITY OF THE
ORIGINAL PAGE IS POOR

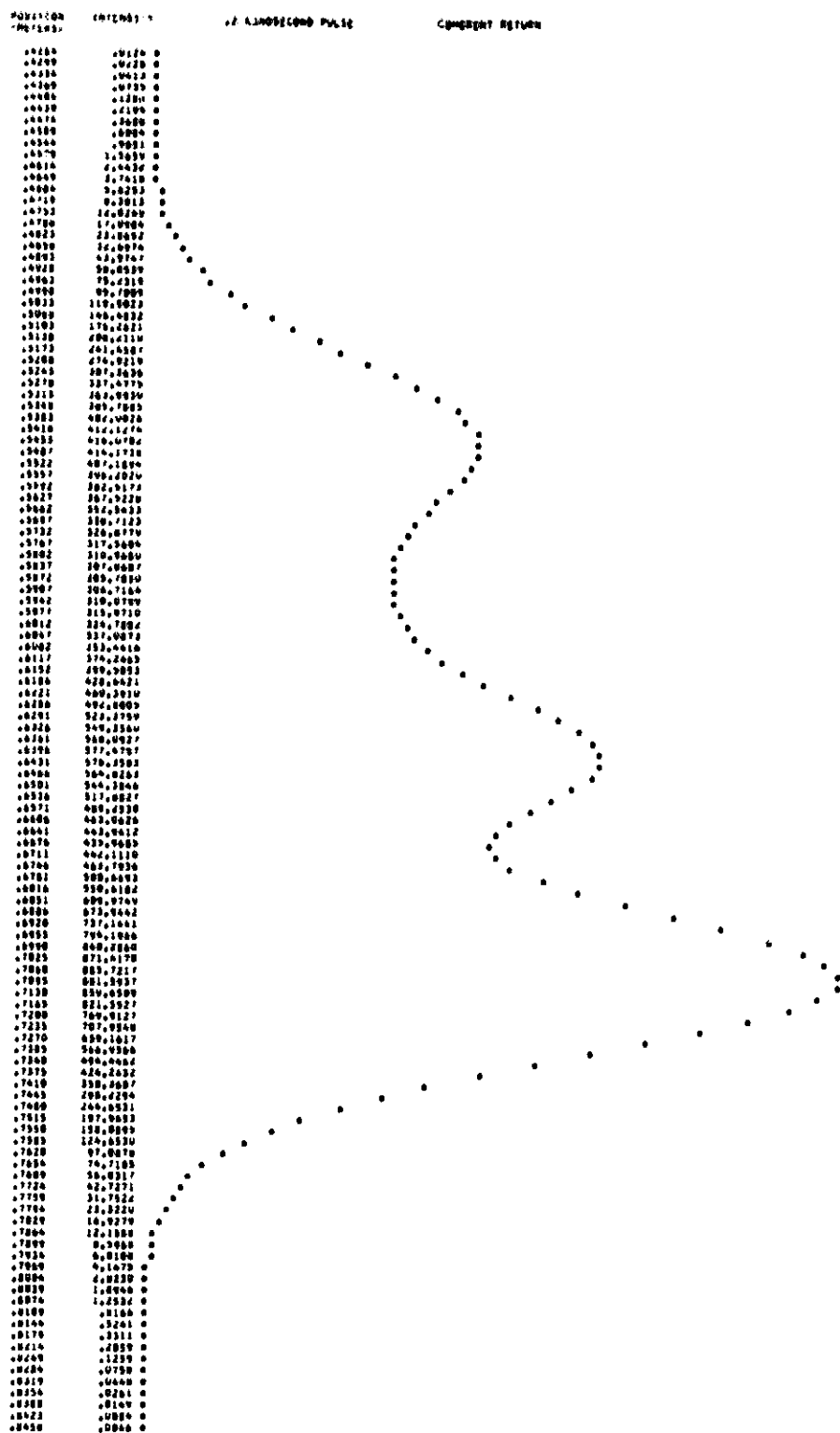


Figure 3g.



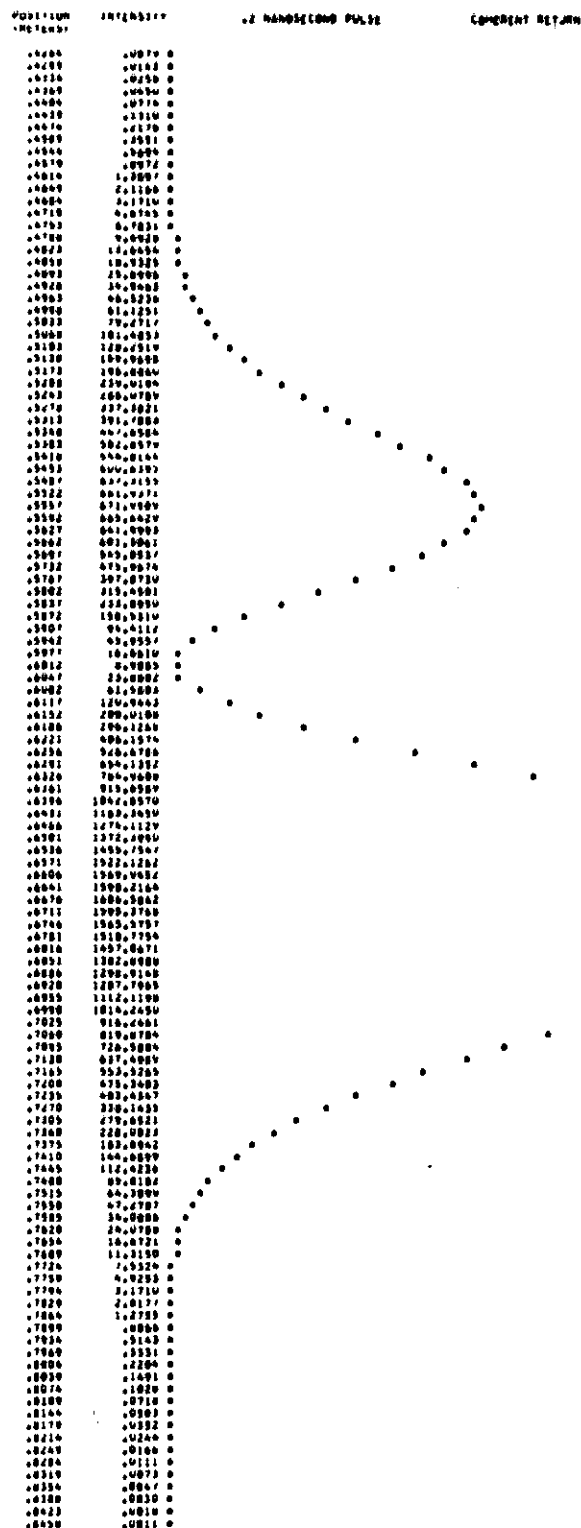


Figure 3i.

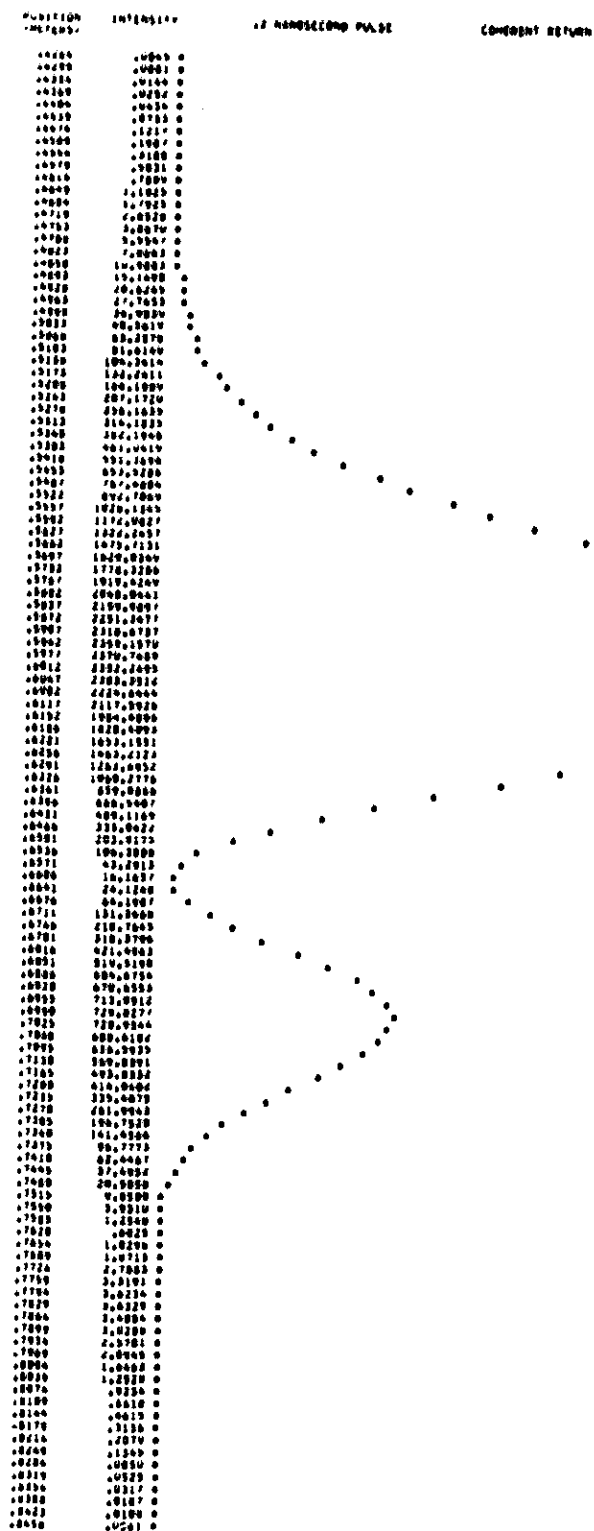


Figure 3j.

11. VARIATIONS IN PULSE CENTROID DUE TO OPTICAL COHERENCE

The interference between the reflections from different cube corners causes the measured range to the array to fluctuate from pulse to pulse. In order to estimate the magnitude of this variation, sets of coherent returns have been calculated for various pulse lengths and incidence angles on the array, and the results are shown in Table 7. Each root-mean-square (rms) deviation was computed from a sample of 100 coherent returns. In Table 7a, all pulses are weighted equally, leading to results that are somewhat erratic owing to the fact that very weak reflected pulses tend to have much larger variations in centroid than stronger pulses do. Each pulse in Table 7b has been weighted by the ratio of the strength of the pulse to the strength of an average (or incoherent) pulse. This procedure gives lower and more consistent rms deviations.

PRECEDING PAGE BLANK NOT FILMED

Table 7a. Coherent range variations, with equal weighting.

20 NANOSECOND PULSE

PHI (DEG)	R.M.S. DEVIATION OF RANGE CORRECTION(METERS)
0.0	0.0000 *
5.0	.0111 *
10.0	.0330 *
15.0	.0873 *
20.0	.0480 *
25.0	.1437 *
30.0	.0627 *

5 NANOSECOND PULSE

PHI (DEG)	R.M.S. DEVIATION OF RANGE CORRECTION(METERS)
0.0	0.0000 *
5.0	.0130 *
10.0	.0268 *
15.0	.0348 *
20.0	.0623 *
25.0	.0696 *
30.0	.0524 *

.2 NANOSECOND PULSE

PHI (DEG)	R.M.S. DEVIATION OF RANGE CORRECTION(METERS)
0.0	0.0000 *
5.0	.0058 *
10.0	.0092 *
15.0	.0120 *
20.0	.0160 *
25.0	.0181 *
30.0	.0202 *

Table 7b. Coherent range variations, weighted by signal strength.

20 NANOSECOND PULSE

PHI (DEG)	R.M.S. DEVIATION OF RANGE CORRECTION(METERS)
0.0	0.0000 *
5.0	.0053 *
10.0	.0119 *
15.0	.0188 *
20.0	.0267 *
25.0	.0350 *
30.0	.0339 *

5 NANOSECOND PULSE

PHI (DEG)	R.M.S. DEVIATION OF RANGE CORRECTION(METERS)
0.0	0.0000 *
5.0	.0062 *
10.0	.0129 *
15.0	.0188 *
20.0	.0265 *
25.0	.0335 *
30.0	.0309 *

.2 NANOSECOND PULSE

PHI (DEG)	R.M.S. DEVIATION OF RANGE CORRECTION(METERS)
0.0	0.0000 *
5.0	.0048 *
10.0	.0082 *
15.0	.0110 *
20.0	.0151 *
25.0	.0182 *
30.0	.0208 *

12. ACCURACY OF RANGE CORRECTION

At normal incidence, the distance to each cube corner is the same, since the array consists of a single plane of retroreflectors. Therefore, the range error introduced by the satellite is only that caused by mechanical uncertainties. Since the distance from the satellite center of mass to the front face is 13.6 ± 0.03 inches, the range uncertainty at normal incidence is 0.03 inch (0.8 mm). At other incidence angles, the cube corners have a spread in range that increases with incidence angle. Since all cube corners have the same orientation, the strength of the reflection from each cube corner should be the same at any viewing angle, and if this is true, the range error at any angle is simply the mechanical uncertainty. The only circumstance under which the range uncertainties could be greater is when the diffraction patterns of individual cube corners vary as a result of different manufacturing procedures or thermal conditions. Testing of the cube corners at GSFC indicates that all the cube corners are very close to diffraction-limited. No information is available on the thermal behavior of the retroreflectors.

The spread in range to individual cube corners forms an upper bound to the possible systematic error introduced by the satellite. The radius of the array is about 20 cm, and the maximum angle of incidence on the array is about 18° if there are no large oscillations of the satellite. Therefore, the maximum spread in range of the cube corners from the center of the array is $20 \times \sin 18^\circ = 6$ cm.

The random-range variations due to coherent interference are about 2 cm at an incidence angle of 18° , according to Table 7b. Since coherent interference is equivalent to very large variations in the reflectivity of individual cube corners, we expect the range uncertainties from other causes to be even smaller than the coherent variations. Therefore, the systematic range error introduced by the array is probably on the order of 1 cm or less.

PRECEDING PAGE BLANK NOT FILMED

13. ACKNOWLEDGMENTS

We wish to express our appreciation to P. O. Minott, of Goddard Space Flight Center; R. Eastern of the Naval Research Laboratory; and H. DeWall of Fairchild Space and Electronics Company for providing information used in this report.

PRECEDING PAGE BLANK NOT FILMED